Clinical Cancer Research

Disulfiram when Combined with Copper Enhances the Therapeutic Effects of Temozolomide for the Treatment of Glioblastoma

Xueqing Lun[1,2], J. Connor Wells[1], Natalie Grinshtein[3], Jennifer C. King[1,2], Xiaoguang Hao[1,2], Ngoc-Ha Dang[1,2], Xiuling Wang[1,2], Ahmed Aman[4], David Uehling[4], Alessandro Datti[5,6], Jeffrey L. Wrana[5,7], Jacob C. Easaw[2,11], Artee Luchman[9], Samuel Weiss[8,9], J. Gregory Cairncross[1,2,10], David R. Kaplan[3,7], Stephen M. Robbins[1,2,11], and Donna L. Senger[1,2,11]

Abstract

Purpose: Glioblastoma is one of the most lethal cancers in humans, and with existing therapy, survival remains at 14.6 months. Current barriers to successful treatment include their infiltrative behavior, extensive tumor heterogeneity, and the presence of a stem-like population of cells, termed brain tumor–initiating cells (BTIC) that confer resistance to conventional therapies.

Experimental Design: To develop therapeutic strategies that target BTICs, we focused on a repurposing approach that explored already-marketed (clinically approved) drugs for therapeutic potential against patient-derived BTICs that encompass the genetic and phenotypic heterogeneity of glioblastoma observed clinically.

Results: Using a high-throughput *in vitro* drug screen, we found that montelukast, clioquinol, and disulfiram (DSF) were cytotoxic against a large panel of patient-derived BTICs. Of these compounds, disulfiram, an off-patent drug previously used to treat alcoholism, in the presence of a copper supplement, showed low nanomolar efficacy in BTICs including those resistant to temozolomide and the highly infiltrative quiescent stem-like population. Low dose DSF-Cu significantly augmented temozolomide activity *in vitro*, and importantly, prolonged *in vivo* survival in patient-derived BTIC models established from both newly diagnosed and recurrent tumors. Moreover, we found that in addition to acting as a potent proteasome inhibitor, DSF-Cu functionally impairs DNA repair pathways and enhances the effects of DNA alkylating agents and radiation. These observations suggest that DSF-Cu inhibits proteasome activity and augments the therapeutic effects of DNA-damaging agents (temozolomide and radiation).

Conclusions: DSF-Cu should be considered as an adjuvant therapy for the treatment of patients with glioblastoma in both newly diagnosed and recurrent settings. *Clin Cancer Res; 1–16. ©2016 AACR.*

[1]Arnie Charbonneau Cancer Institute, University of Calgary, Calgary, Alberta, Canada. [2]Clark H. Smith Brain Tumour Centre, University of Calgary, Calgary, Alberta, Canada. [3]Program in Neurosciences and Mental Health, The Hospital for Sick Children, Toronto, Ontario, Canada. [4]Drug Discovery Platform, Ontario Institute for Cancer Research, Toronto, Ontario, Canada. [5]Lunenfeld-Tanenbaum Research Institute, Mount Sinai Hospital Toronto, Ontario, Canada. [6]Department of Agricultural, Food, and Environmental Sciences, University of Perugia, Perugia, Italy. [7]Department of Molecular Genetics, University of Toronto, Ontario, Canada. [8]Hotchkiss Brain Institute, University of Calgary, Calgary, Alberta, Canada. [9]Department of Cell Biology & Anatomy, University of Calgary, Calgary, Alberta, Canada. [10]Department of Clinical Neurosciences, University of Calgary, Calgary, Alberta, Canada. [11]Department of Oncology, University of Calgary, Calgary, Alberta, Canada.

Note: Supplementary data for this article are available at Clinical Cancer Research Online (http://clincancerres.aacrjournals.org/).

X. Lun and J.C. Wells are co-first authors of this article.

S.M. Robbins and D.L. Senger share senior authorship.

Corresponding Authors: Donna L. Senger, Arnie Charbonneau Cancer Institute, University of Calgary, Rm362 Heritage Medical Research Building, 3330 Hospital Drive, NW, Calgary, Alberta T2N 4N1, Canada. Phone: 403-220-8693; Fax: 403-210-8135; E-mail: senger@ucalgary.ca; and Stephen M. Robbins, srobbins@ucalgary.ca

doi: 10.1158/1078-0432.CCR-15-1798

Introduction

Grade IV glioma and glioblastoma are the most lethal and aggressive forms of brain tumors in adults. Despite treatment advances combining maximal surgical resection with radiotherapy and concurrent and adjuvant chemotherapy (temozolomide), patient prognosis remains disappointing and survival is limited to 14.6 months with few cases of long-term survivors (1). Current barriers to successful treatment include their complex tumor heterogeneity, diffuse invasiveness, and the presence of a subpopulation of glioma cells with stem-like properties, herein termed brain tumor–initiating cells (BTIC; refs. 2, 3), that have been shown to confer resistance to conventional therapies, such as radio- and chemotherapies (4–8). Thus, to improve clinical outcomes, therapeutic agents should target both the infiltrative and tumor-initiating disease reservoirs.

Temozolomide is the current standard-of-care chemotherapy for glioblastoma. Although it improves the survival of patients, especially in the context of methylation of the O6-methylguanine DNA methyltransferase (MGMT) locus (9), the survival benefit remains unsatisfactory and temozolomide resistance is common in the clinic (6, 10). To improve the survival of glioblastoma patients, new therapeutic strategies including combination-based therapies are desperately needed. We have been investigating the

Translational Relevance

Malignant glioma is one of the most common primary central nervous system tumors and improvement in overall survival has been incremental. Major barriers to effective treatment of glioblastoma are their highly invasive, tumorigenic, and "stem cell–like" characteristics. To improve clinical outcomes, new therapeutic strategies are needed. Using both *in vitro* and *in vivo* models, we found that the off-patent drug disulfiram (DSF) when chelated with copper and administered with standard-of-care temozolomide (Temodar) was a highly effective therapeutic for newly diagnosed, recurrent, and temozolomide-resistant glioblastoma. Moreover, we determined that the increase in therapeutic activity, in part, results from the downregulation of genes involved in DNA repair that augment the effects of DNA alkylating agents and radiation treatment. Herein we provide strong rationale for the clinical use of DSF-Cu in combination with current standard-of-care in newly diagnosed and in patients with recurrent tumors that have acquired resistance to temozolomide.

treatments that are adjunctive to current standard-of-care and enhance the cytotoxicity of temozolomide using BTICs established from newly diagnosed and recurrent glioblastoma patients (2, 3, 11–13) as the screening platform. These cells retain cardinal features of stem cells including the ability to self-renew and differentiate into multiple neural cell lineages (2, 3). They also have signature characteristics of transformed cells such as growth factor independence, tumorigenicity, and a spectrum of molecular genetic alterations known to occur in glioblastoma (e.g., p53, PTEN, IDH1, EGFR; refs. 2, 3, 13). These highly tumorigenic cells form tumors *in vivo* that look and behave like glioblastoma including infiltration of the cerebral cortex and spreading along the subependyma and corpus callosum (3). Using a high-throughput *in vitro* drug screen with two chemical libraries (NIH; ToolKit) we identified three candidate compounds, clioquinol, montelukast, and disulfiram for initial preclinical assessment. We found that DSF, an off-patent drug (FDA-approved) that crosses the blood brain barrier (BBB), had low nanomolar efficacy against patient-derived BTICs (including the highly infiltrative disease reservoir) when combined with copper gluconate and thus warranted further investigation.

Recently, several independent groups, including this study, have identified DSF through high-throughput screens as a potential therapeutic for the treatment of various cancers including glioblastoma (14–19). As DSF has been used clinically for over 60 years to treat alcoholism, its pharmacokinetics has been extensively studied and shown to have an excellent safety record at FDA-recommended doses (20, 21). DSF is available, inexpensive, safe, and overall well-tolerated making it an attractive candidate for "repurposing" in the context of glioblastoma. Although the anticancer mechanisms of DSF are still not well-understood (22), published data indicate that the cytotoxicity of DSF is enhanced in the presence of copper (14, 15, 23). DSF chelates bivalent metals such as copper (Cu) and zinc (Zn) to form DSF metal complexes that inhibit proteasome activity and block the degradation of IκB and NFκB nuclear translocation (24–26). In the clinical situation, DSF combined with zinc gluconate has resulted in remission in a melanoma patient with liver metastasis (27). The importance, however, of a bivalent metal such as copper for DSF's mechanistic action in the context of glioma, and specifically against the BTIC population, has not been examined.

In this study, we evaluated the use of DSF as a potential therapeutic drug for glioblastoma using a combination of *in vitro* and *in vivo* preclinical models. We demonstrate that in addition to being a potent proteasome inhibitor, DSF when chelated with copper downregulates the expression of a number of genes involved in DNA repair pathways. Consistent with this observation, we found that DSF-Cu enhanced the DNA-damaging effects of temozolomide, BCNU, and radiation (IR) *in vitro* and in combination with temozolomide prolonged survival in newly diagnosed, recurrent, and temozolomide resistant intracranial patient-derived BTIC models *in vivo*. Our observations suggest that as a single agent, DSF-Cu has limited *in vivo* efficacy; however, when given in the context of a DNA alkylating agent (temozolomide or BCNU) and/or DNA-damaging agent (IR), DSF-Cu has the potential to be repurposed for the treatment of patients with highly infiltrative glioma.

Materials and Methods

BTIC lines, tissue culture, and reagents

Surgical samples from patients with newly diagnosed and recurrent glioblastoma were obtained from the Tumor Tissue Bank within the Arnie Charbonneau Cancer Institute (Calgary, Alberta, Canada), transported to the BTIC Core Facility (Calgary, Alberta, Canada) and established as described previously (2, 3, 13). All established cell lines used within this study were validated for identity by short tandem repeat analysis performed by Calgary Laboratory Services (CLS) after each thaw and for each experiment that involved intracranial xenografts. This study has Institutional review board approval under the "Brain Tumor and Related Tissue Bank protocol-V2" and approved by Foothills Hospital and the Conjoint Health Research Ethics Board.

Stable BTIC lines expressing enhanced firefly luciferase (effLuc) and eGFP were generated using a self-inactivating lentiviral vector system as described previously (28, 29). BT73R and BT206R are temozolomide-resistant BTIC lines generated from parental BT73 and BT206. Briefly, BT73- and BT206-expressing effLuc/eGFP were implanted into the brain of CB17 SCID mice (Charles River Laboratory) and two weeks after implantation, animals were treated with a temozolomide regime of 50 mg/kg/day (one cycle) followed by 5 cycles of 10 mg/kg/day (cycle = 5 days on, 2 days off). Animals were monitored for recurrence at which time tumors were removed, dissociated, cultured under neurosphere conditions, and reimplanted into animals. Two weeks after the appearance of a recurrent tumor, animals were treated with a temozolomide regime of 50 mg/kg/day (one cycle) followed by 30 mg/kg/day (two cycles). Upon recurrence, tumor tissue was dissociated and cultured in neurosphere media. The derived temozolomide -resistant lines were termed BT73R and BT206R.

NIH clinical drug collection consists of 446 small-molecule compounds that have a history of use in human clinical trials. The library was purchased from Evotec Inc. The ToolKit library was provided by the Ontario Institute for Cancer Research (Toronto, Canada) and included 160 compounds. Disulfiram was purchased from AKT laboratories, montelukast was purchased from Gibco Life Technologies, copper (II) gluconate, clioquinol, and

temozolomide were purchased through Sigma. Clinical grade Velcade (bortezomib) was obtained from the Tom Baker Cancer Centre (Calgary, Alberta) and was dissolved in normal saline (0.9% w/v NaCI). Clinical grade disulfiram (Antabuse; Odyssey Pharmaceuticals) and the copper supplement, copper bisglycinate (M228) were purchased from Thorne Research.

The following antibodies were used for Western blot analysis and IHC: mAbs against human nestin (R&D Systems, cat# MAB1259), human nucleolin (4E2, Abcam; cat# ab13541); phospho-histone H2AX (Ser139, clone JBW301; Millipore cat# 05-636); MGMT (Novus Biologicals, cat# NB100-168); β-actin (clone C4, EMD Millipore; cat# MAB1501); and polyclonal antibodies against MGMT (NEB, cat# 2739); PARP (Cell Signaling Technology, cat# 9542); Phosph-Ser 345 Chk1 (Cell Signaling Technology, cat# 2341), and Chk1 (Cell Signaling Technology, cat# 2360).

High-throughput screening and secondary validation

High-throughput screening was performed at the SMART Facility of the Lunenfeld-Tanenbaum Research Institute (Toronto, Canada), as described previously (30, 31). Drug "hits" were defined as compounds that caused a signal decrease of at least 75% at a screening dose of 1 μmol/L as compared with controls. Compounds that exhibited greater than 50% but lower than 74% cytotoxicity were considered "intermediate potency hits." Secondary validation was performed on a subset of BTICs using 8-point, 3-fold serial dilutions of compounds.

For DSF viability assessment by AlamarBlue, cells were treated as indicated at the concentrations delineated in the text at 24 to 72 hours with the exception of temozolomide where viability was assessed on day 10. Five replicates per treatment were assessed and each experiment was repeated at least twice.

Self-renewal assay

BTIC self-renewal (secondary sphere-forming) assays were performed under neural stem cell conditions as described previously (3, 32). Spheres were dissociated and viable cells were counted. Ten or 100 cells were then placed into 96-well plates and cultured for an additional 7 days, and secondary sphere formation was counted. Spheres >30 μm were counted and photographed using a Zeiss Axiovert 200M inverted fluorescent microscope and AxioCam MRc camera.

Apoptosis assay

Apoptotic status was determined by FITC-conjugated Annexin-V/PI assay kit (Roche) using flow cytometry following the manufacturer's instructions at 24 and 48 hours. Cells stained with Annexin V only were classified as cells undergoing early apoptosis and the Annexin V and PI double–stained cells were classified as cells in late apoptosis or necrosis. Whole brain sections were assessed for apoptosis using terminal deoxynucleotidyl transferase–mediated dUTP nick end labeling (TUNEL) to detect DNA fragmentation using InSitu Cell Death Detection Kit, Fluorescein (Roche Life Science, cat# 11684795910) following manufacturer's protocol. Sections costained for DNA damage were subsequently incubated with anti-phospho-histone H2AX (Ser139, clone JBW301) and secondary Alexa Fluor 488–conjugated goat anti-mouse lgG and counterstained with 4′,6-diamidino-2-phenylindole (DAPI; blue) to visualize the nuclei.

Western blot analysis

Cells were harvested following treatment, washed with PBS, and sonicated in 50 nmol/L Tris-HCI (pH 8.0) containing 1% glycerol, 1 mmol/L EDTA, 0.5 mmol/L phenylmethylsulfonylfluoride, and 2 mmol/L benzamidine. Equal protein amounts were subjected to SDS-PAGE, transferred to nitrocellulose, and Western blot analysis was performed as described previously (33, 34) using the appropriate primary and secondary antibodies.

Chymotrypsin-like (26S) activity proteasome assay

Chymotrypsin-like (CT) activity (26S activity) was measured using the CT-like proteasome-Glo assay (Promega) at 24 or 72 hours following treatment. Luminescence was measured using a luminometer (SpectraMax) and activity was reported as the mean percent activity compared with control.

For *in vivo* analysis of 26S proteasome activity, animals bearing BTIC intracranial tumors were treated with vehicle (Oral Plus), DSF, or DSF-Cu for 5 and 10 days; following treatment, animals were sacrificed, tumor tissue was collected, and 26S proteasome activity was assessed using the proteasome activity assay (ab107921; Abcam).

GammaCell irradiation

Cells grown on laminin (L202; Sigma) coated coverslips or plated in 6-cm plates were either untreated or treated with DSF-Cu (50 nmol/L DSF; 200 nmol/L Cu) 12 hours before irradiation treatment. Following the 12-hour pretreatment, cells were either untreated, treated with [(10 μg/mL, (51.5 μmol/L) TMZ] or irradiated using a GammaCell 1000 Elite Tissue Irradiator (dose rate 2.94 Gy/minute, 41 seconds to deliver a dose of 2 Gy to cells on coverslips, and 102 seconds to deliver a dose of 5 Gy to cells in 6-cm plates) followed by recovery at 37°C for the indicated time points (hours).

Immunofluorescence and assessment of DNA damage

Cells grown on 8-well chamber slides or laminin (L202; Sigma) coated coverslips were fixed in 4% paraformaldehyde and permeabilized with addition of 0.1% Triton-X100 prior to immunostaining. Primary mouse monoclonal anti-phospho-histone H2AX (Ser139, clone JBW301) and secondary Alexa Fluor 488–conjugated goat anti-mouse lgG were sequentially applied. For whole brain tissue sections, paraffin-embedded tissues were deparaffinized with xylene, rehydrated through an ethanol gradient, and treated as described previously (33) to staining with anti-phospho-histone H2AX. Nuclei were counterstained with 2 μg/mL of DAPI and chambers were removed and coverslips were mounted onto the glass slides. DNA damage was visualized by immunofluorescence microscopy using the InCell 6000 (GE Healthcare Life Sciences) or a Zeiss platform microscope (Axio Observer.ZI; Carl Zeiss), with a Plan Apochromat 20×/0.8 NA, an EC Plan Neofluar 40×/0.75 NA, or a Plan Apochromat 63×/1.4 NA (oil immersion) objective and camera (AxioCam MRm Rev.3; Carl Zeiss). Acquisition and analysis software used was Zen Pro (Carl Zeiss). DNA damage was assessed by manual foci counting.

Microarray

RNA was extracted from 500,000 cells treated for 12 hours (as indicated) using mirVana miRNA Isolation Kit (Ambion) according to the manufacturer's protocol. Total RNA was purified with

RNeasy Plus Micro Kit (Qiagen) and RNA integrity number (RIN) was measured using the Agilent RNA 6000 NanoChip on 2100 Bioanalyzer (Agilent Technologies). Quantity was measured using NanoDrop 1000 (NanoDrop Technologies, Inc) and 100 ng of RNA with a RIN higher than 9 was labeled with 3′ IVT Express Kit (Ambion) and hybridized to Affymetrix GeneChip Human PrimeView Arrays at 45°C for 16 hours. Arrays were stained using Affymetrix GeneChip Fluidics_450 following manufacturer's protocol and scanned using the Affymetrix GeneChip Scanner 3000 7G System. The raw datasets for array comparisons have been deposited in the Gene Expression Omnibus website (http://www.ncbi.nlm.nih.gov.geo/; accession number, GSE76146).

Microarray data analysis

Affymetrix GeneChip array data files were generated using GeneChip Command Console Software (AGCC) and statistical analysis was carried out using Partek Genomics Suite 6.0 (Partek Incorporated, USA). Of the 20,000 genes represented on the array, the fold change was calculated as compared with control. To categorize biologic functions related to gene expression altered by DSF-Cu treatment, fold-change files were uploaded into DAVID Bioinformatics Resources 6.7 (National Institute of Allergy and Infectious Diseases, NIH, Bethesda, MD).

***In vivo* experiments**

Six- to 8-week-old female SCID mice (CB17) from Charles River Laboratory were used in this study. All protocols were reviewed and approved by the Animal Care Committee of the independent laboratory and the University of Calgary (Calgary, Alberta, Canada). All animal work procedures were in accordance with the Guide to the Care and Use of Experimental Animals published by the Canadian Council on Animal Care and the Guide for the Care and Use of Laboratory Animals issued by NIH (Bethesda, MD).

Characterization of BTICs *in vivo*

Patient-derived BTICs from newly diagnosed (BT73, BT108, BT126, BT127, BT134, BT164) and recurrent (BT119, BT143, BT147) tumors were implanted into the brain of mice as described previously (3, 32, 34). Mice were monitored weekly and tumor growth was assessed using the IVIS-200 Optical *in vivo* imaging system, MRI, or by IHC at designated timepoints. Immunohistochemical assessment was performed after formalin fixation, paraffin embedding, and sectioning of the brains. All sections were stained with hematoxylin and eosin (Eosin, Anatech Ltd, cat# 832) and IHC was performed using human-specific mAbs against nestin (1/200), human nucleolin (R&D Systems; 1:500), γ-H2AX (1/100) at 4°C overnight and detected using DAKO Envision and System-HRP Kit (cat# K4007). Slides were counterstained with hematoxylin (Sigma, cat# GHS232-1L), mounted, and imaged using a Zeiss inverted microscope (Axiovert 200M) and camera (AxioCam MRc).

***In vivo* efficacy studies**

In vivo efficacy studies were determined by stereotactically implanting 1×10^5 BTIC cells into the right striatum of SCID mice (Charles River Laboratory; refs. 3, 32). Tumors were allowed to grow for 7 days at which time animals were treated as follows: clioquinol was administered daily via intraperitoneally injection to animals bearing intracranial BT147 tumors at a concentration of 15 mg/kg clioquinol in 20% intralipid once per day or twice per day for 4 cycles (5 days on, 2 days off). Montelukast was administered daily via intraperitoneal injection to animals bearing intracranial BT147 tumors at a concentration of 25 mg/kg montelukast in H_2O once per day for 3 cycles (5 days on, 2 days off). DSF-Cu and/or temozolomide, was administered to mice with intracranial patient-derived BTIC tumors (BT73, BT73R, BT134, and BT147) by oral gavage. Treatment groups included Oral Plus (vehicle control); DSF-Cu [DSF, 100 mg/kg/daily, copper (Cu) 2 mg/kg/daily]; temozolomide (50 mg/kg/mouse/daily), or temozolomide plus DSF-Cu via gavage starting 7 days after tumor implantation. DSF and Cu were delivered as separate formulations via gavage. Animals were treated for 3 cycles with each cycle consisting of 5 days of treatment followed by two nontreatment days. All treatment groups consisted of 8–12 animals as indicated. Animals were monitored and imaged weekly for tumor burden by bioluminescence using the IVIS-200 Optical *in vivo* imaging system, by MRI using 9.4 T NMR instrument in the Experimental Imaging Center (University of Calgary, Calgary, Alberta, Canada) or by IHC of formalin-fixed, paraffin-embedded whole brain sections. Animals assessed for survival were monitored until they lost $\geq$20% of body weight or had trouble ambulating, feeding, or grooming, or until the experiment was terminated.

Statistical analysis

Statistical Analysis Software (SAS Institute, Inc.) and GraphPad Prism (version 4; GraphPad Software, Inc.) were used for statistical analyses. Survival curves were generated using the Kaplan–Meier method. The log-rank test was used to compare the distributions of survival times. A P value of less than 0.05 was considered statistically significant. Experimental data was collected from multiple experiments and reported as the treatment mean $\pm$ SE. Significance was calculated using the Student t test or one-way ANOVA where *, $P < 0.05$ and **, $P < 0.01$ or as indicated.

Results

Screening BTICs for cytotoxicity to clinically approved drugs

To screen for drugs that could prevent the proliferation and survival of BTICs, we performed a primary screen with the NIH clinical drug library (Evotec, Inc.) that contains 446 compounds that have been used in human clinical trials, and a ToolKit library (Ontario Institute for Cancer Research, Toronto, Ontario, Canada) containing 160 compounds against 13 independent genetically distinct patient-derived BTIC lines (BT-12, 25, 50, 53, 67, 68, 73, 84, 89, 108, 119, 124, 147) cultured using standard neurosphere conditions (refs. 3, 13, 32, 35; described in Fig. 1A and ref. 30). On the basis of established genetic alterations observed in glioblastoma, the panel of BTICs screened was chosen to encompass the molecular heterogeneity of the disease as assessed by mutational status of EGFR, PTEN, p53, and MGMT promoter methylation status and were derived from both newly diagnosed and recurrent tumors (summarized in Supplementary Table S1; refs. 2, 3, 13). Compounds were identified that exhibited more that 50% growth inhibition at 1 μmol/L in all BTIC cultures using AlamarBlue reduction as we have previously described (30, 31). Compounds that exhibited greater than 50% but lower than 74% cytotoxicity were considered "intermediate potency hits" and indicated in yellow while compounds demonstrating greater than 75% growth inhibition were defined as "strong hits" and indicated in green (Fig. 1B and C). To validate the compounds identified from the

primary screens, a secondary independent screen with a random selection of BTICs was performed using 8-point serial dilutions and the IC_{50} for each compound was calculated. On the basis of the relatively large number of hits (30 drugs), compounds were further prioritized on the basis of showing efficacy on most or all primary-BTIC lines and on their ability to cross the blood–brain barrier (BBB). Many compounds from the list, such as idarubicin, doxorubicin, epirubicin, clofazimine, dactinomycin, bortezomib, and ouabain were reported to not cross the BBB and were therefore not pursued further. To prioritize among the remaining compounds, we used six criteria (summarized in Supplementary Table S2): (i) efficacy on BTICs *in vitro*; (ii) potency *in vitro* (nanomolar to low micromolar); (iii) BBB penetration and brain accumulation; (iv) clinical status; (v) toxicity to normal cells; and (vi) novelty. From the prioritized list, the top candidates were assessed in a secondary screen performed on a subpanel of patient-derived BTICs using 8-point serial dilutions (Supplementary Figs. S1A, S2B, and S3). From these candidate compounds, we chose montelukast, a leukotriene receptor antagonist used for the treatment of acute asthma (36, 37), clioquinol, a hydroxyquinoline that has been used as an antifungal and antiprotozoal drug (38), and disulfiram, an off-patent drug previously used to treat alcoholism (21, 39) for further assessment. While *in vitro* studies were validated for clioquinol (Supplementary Fig. S1A), and it was found to

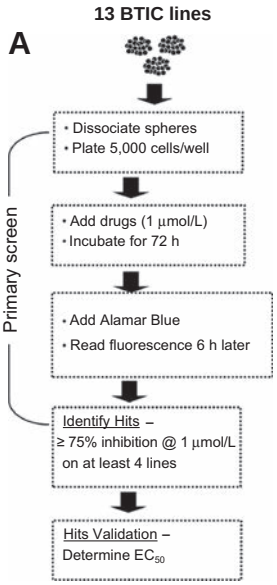

B

BTIC lines

Drug	Indication/target	BT12	BT25	BT50	BT53	BT67	BT68	BT73	BT84	BT89	BT108	BT119	BT124	BT147
Idarubicin	Chemotherapy													
Doxorubicin														
Epirubicin														
Cerivastatin	Statins													
Mevastatin														
Itavastatin														
Clofazimine	Anti-bacterial													
Dactinomycin	Antibiotic													
Oxiconazole nitrate	Anti-fungal													
Bifonazole	Anti-fungal													
Disulfiram	ALDH													
Triptolide	NFκB inhibitor													
Montelukast	LTRA													
MK-866	FLAP inhibitor													
Homoharringtonine	Cytotoxic alkaloid													
Benzbromarone	Uricosuric agent													
Amiodarone	Anti-arrhythmic agent													
Ebselen	Potent scavenger of H2O2													
Glycopyrrolate	Blocks muscarinic receptors													
Palonosetron	5HT3 receptor antagonist													
Nonyloxytryptamine	Selective SR-1B agonist													
Chloro-2-deoxyadenosine	Inhibits DNA synthesis													

C

BTIC lines

Drug	Indication/target	BT12	BT25	BT50	BT53	BT67	BT68	BT73	BT84	BT89	BT108	BT119	BT147
Clioquinol	Metal chelator												
NIH, 311													
GX15-070 (Obatoclax)	BCL2												
TW37													
ABT-263													
ABT-737													
YM-155	Survivin												
Sertaconazole nitrate	Anti-fungal												
Econazole nitrate													
Butoconazole													
Cercosporin	Phototoxin												
KRIBB3	HSP27												
17-AAG	HSP-90												
17-DMAG													
Bortezomib	proteasome												
Ouabain	Na+, K+ ATPase												
Anisomycin	antibiotic												
AGK2	SIRT2												
Anilinoquinoline	Guanylate cyclase												

Figure 1.

High-throughput drug screen for compounds that show low nanomolar efficacy against patient-derived BTICs identifies disulfiram. A–C, 13 genetically distinct patient-derived BTICs (BT-12, 25, 50, 53, 67, 68, 73, 84, 89, 108, 119, 124, 147) established under standard neurosphere conditions were screened using the NIH Clinical Compound Library (B) and ToolKit (C) as described previously (30). A, schematic outlines the high-throughput screen. BTICs were dissociated into single cells and seeded at 5,000 cells/well in 100-μL medium in 96-well microplates. Compounds were dissolved in DMSO, realiquotted in daughter plates as 1 mmol/L solutions, and added using a pin tool to achieve a final concentration of 1 μmol/L. Drug effects were compared with cells optimally proliferating in 0.1% DMSO alone, while wells filled with media served as background. AlamarBlue (10 μL) was added after 72 hours, and fluorescence intensity measured after 6 hours on a PHERAstar microplate reader, equipped with a l540 excitation/ l590 emission filter. B and C, tables show compounds from NIH (B) and Toolkit (C) libraries that exhibited greater than 50% (yellow) or 75% (green) growth inhibition at 1 μmol/L in all 13 BTIC cultures as compared with controls. (*Continued on the following page.*)

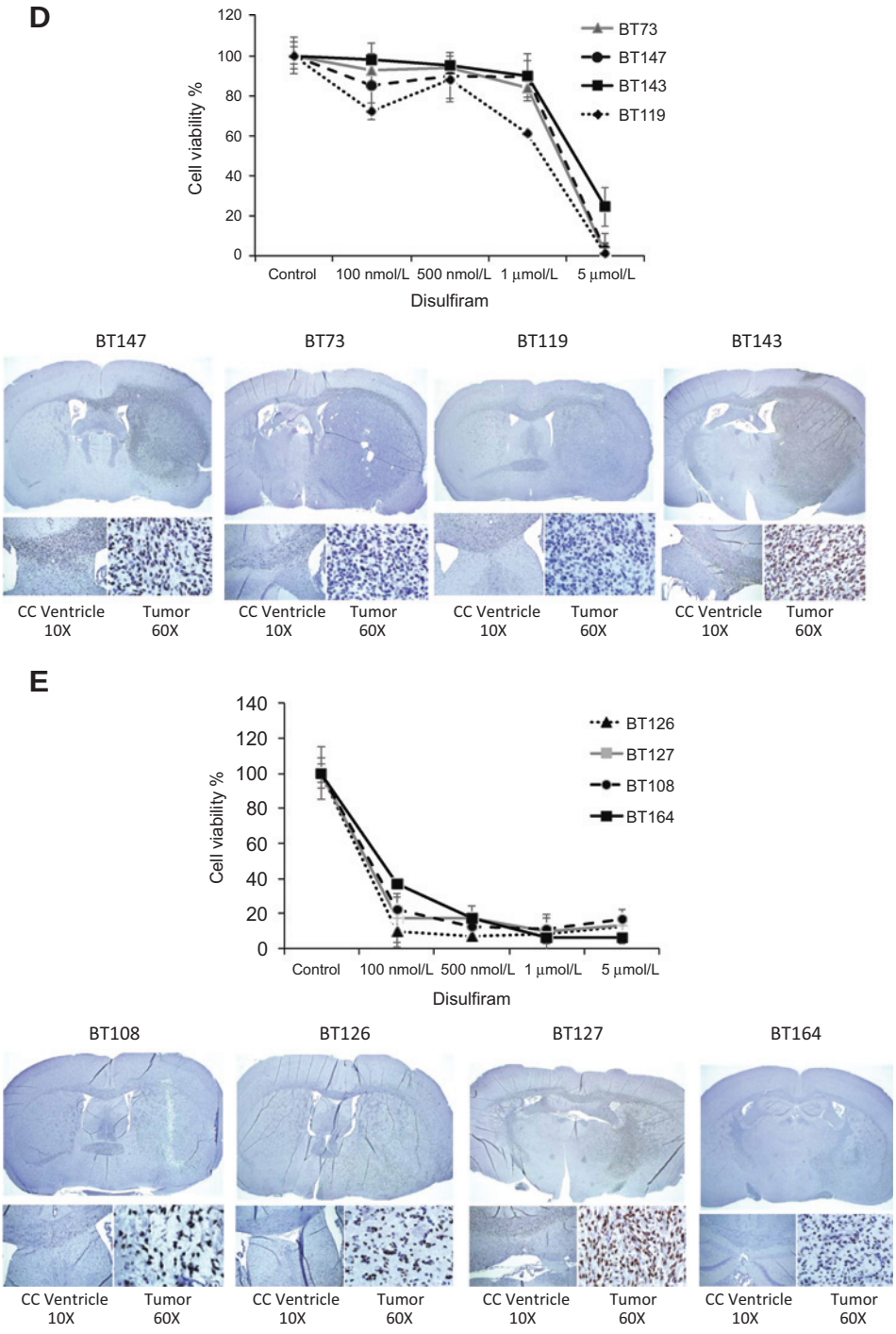

Figure 1.
(*Continued.*) D and E, secondary screening of disulfiram on BTICs established from newly diagnosed (BT73, BT108, BT126, BT127, BT164) and recurrent (BT119, BT143, BT147) patient tumors was performed by treating BTICs with increasing concentration of DSF (100 nmol/L–5 μmol/L). Cell viability was assessed using AlamarBlue and graphs show percent survival after 24 hours of BTICs resistant (D) or sensitive (E) to treatment with DSF alone (top). Whole brain sections (bottom) were stained for anti-human nucleolin (brown) and confirmed *in vivo* tumorigenicity of all BTICs tested (bottom). Sections were counterstained with hematoxylin (blue).

cross the BBB (Supplementary Fig. S1B), preclinical assessment was halted on the basis of toxicities we observed when administered to mice, and the inability to demonstrate improved survival in a patient-derived intracranial model (BT147; Supplementary Fig. S1C–S1E). Similarly, while montelukast (Supplementary Fig. S2) was validated *in vitro* (Supplementary Fig. S2B and S2D), this compound also showed signs of toxicity as a single agent *in vivo* and failed to demonstrate survival benefit (Supplementary Fig. S2E and S2F). We therefore focused upon further assessment of disulfiram. While the evaluation of DSF is certainly not unique in the cancer setting (14–16, 19, 25, 27, 40), including studies in glioma (17, 41, 42), *in vivo* preclinical assessment for glioblastoma has not been performed. Thus, the independent validation of activity against the patient-derived glioma cells, DSF's low nanomolar efficacy on these cells, BBB penetration, and its extensive multi-decade clinical use with very little evidence of adverse drug reactions made it desirable to pursue in a rigorous preclinical assessment regime.

DSF requires copper for effective killing and inhibition of self-renewal of genetically distinct patient-derived BTICs

As described above, DSF was found to be highly effective at killing a wide range of patient-derived BTICs, an observation consistent with recent *in vitro* reports using human glioma cell lines (17, 18, 41, 43); however, *in vivo* testing has not been performed and discrepancies with respect to the IC_{50} and the requirement of copper for its therapeutic effects exist (17, 18). We found that while some patient-derived BTICs were sensitive to the treatment with DSF alone (Fig. 1E), many of the BTICs including BTICs resistant to treatment with temozolomide (Supplementary Fig. S4; ref. 11) were resistant (Fig. 1D). We confirmed that all BTICs tested were capable of forming tumors *in vivo* (Fig. 1D and E) and found that their sensitivity or resistance to DSF alone *in vitro* was independent of mutational status (p53, EGFR, PTEN), MGMT methylation status, or previous treatment (newly diagnosed vs. recurrent; Supplementary Table S1; refs. 2, 3, 13). Moreover, we found that the addition of copper gluconate (Cu, 200 nmol/L) increased sensitivity and cell killing including BTICs resistant to DSF alone (Fig. 2A and Supplementary Fig. S5A and S5B; **, $P < 0.001$ comparing DSF-Cu with DSF or Cu alone) and significantly inhibited the self-renewal ability (Fig. 2B; **, $P < 0.001$ comparing DSF-Cu with DSF or Cu alone).

DSF-Cu augments the cytotoxic effects of temozolomide and enhances apoptosis

We next determined whether combination therapy with DSF-Cu and standard-of-care temozolomide could promote or enhance efficacy of DSF-Cu *in vitro*. We found that low dose DSF-Cu significantly increased temozolomide cell killing *in vitro* (Fig. 2C and Supplementary Fig. S6A and S6B; **, $P < 0.001$ comparing temozolomide plus DSF-Cu with temozolomide or DSF-Cu alone) and importantly overcame the temozolomide resistance observed in some of the BTIC cell lines including temozolomide-resistant BTIC variants (BT73R and BT206R) established from newly diagnosed patient-derived BT73 and BT206 (Fig. 2E–H). Moreover, this enhancement of BTIC susceptibility in the presence of temozolomide together with DSF-Cu does not rely on the status of MGMT as inhibition of MGMT by O6-benzylguanine (43, 44) did not inhibit the ability of DSF-Cu/temozolomide to decrease cell viability (Supplementary Fig. S7). This is consistent with, DSF-Cu/temozolomide significantly inhibiting cell viability of temozolomide-resistant BTIC variants that either express (BT73R) or do not express (BT206R) MGMT (Fig. 2E), further supporting the notion that DSF-Cu/temozolomide sensitivity can be independent of MGMT status (Supplementary Fig. S7). In addition, DSF-Cu when combined with clinically relevant doses of temozolomide induced more apoptosis than either compound alone as assessed by FACS analysis and PARP cleavage (Fig. 2D and Supplementary Fig. S6D–S6F). This combination benefit is of direct clinical interest given the extensive use of temozolomide in the clinic and the associated problems with temozolomide-related resistance and treatment failure.

DSF inhibits both the proteasome and reduces DNA repair capabilities

DSF has been reported to have several biologic activities including its well-characterized activity as an aldehyde dehydrogenase (ALDH) inhibitor for the treatment of alcoholism, its ability to be an effective proteasome inhibitor (26S), and recently, its ability to inhibit the activity of MGMT (43). Moreover, there is growing literature to suggest that the anticancer properties of DSF do not rely solely on its ability to inhibit ALDH (45), a mechanism that does not require Cu. As we show a requirement for Cu for effective killing of all patient-derived BTICs, we investigated alternative mechanism(s)-of-action. We first investigated the requirement for Cu to inhibit the 26S activity of the proteasome, a mechanism suggested for DSF in other cancers (26). Using both newly diagnosed and recurrent patient-derived BTICs, we found that the addition of Cu was required for DSF to inhibit the 26S proteasome activity (Fig. 3A and B and Supplementary Fig. S8). Moreover, when DSF-Cu was directly compared with the clinically approved proteasome inhibitor bortezomib, we found that bortezomib was not able to elicit the same robust cell death seen with DSF-Cu even at concentrations that completely inhibit the proteasome (Fig. 3A and B). In addition, when BTICs were treated with very low concentrations of DSF-Cu, concentrations where proteasome inhibition was not maximal, DSF-Cu was still able to effectively kill the BTICs (Fig. 3A and B and Supplementary Fig. S8). Thus, inhibition of the proteasome may be responsible for some but not all of the cytotoxicity of DSF-Cu in BTICs.

To identify other mechanisms of action specific to the DSF-Cu complex, we performed global gene expression analysis before and after treatment with DSF, Cu, or DSF-Cu. As expected, when BTICs were treated with Cu alone, we observed the induction of a number of genes in the metallothionein family, which comprise Cu-binding proteins that protect against oxidative stress. In the DSF-Cu–treated cells, we also observed a number of very specific changes in gene expression including the downregulation of a large number of genes, many of which have been implicated in DNA damage and repair pathways both *in vitro* and *in vivo* (Fig. 3C and D; Supplementary Table S3). On the basis of these data, we assessed whether DSF-Cu was able to enhance the DNA damage induced by temozolomide. We found that cells treated with the combination therapy of DSF-Cu and temozolomide had increased DNA damage as assessed by immunostaining and Western blot analysis for γ-H2AX (Fig. 4A–D). These data suggest that the DNA repair pathways were suppressed by DSF-Cu and provide a new mechanism of action to explain the ability of DSF-Cu to enhance the therapeutic effects of temozolomide. Moreover, we found that this augmentation of DNA damage was not limited to temozolomide and was also observed when cells were treated with IR (Fig. 4C–F) where DSF-Cu was found to increase the accumulation of γ-H2AX–positive foci and inhibit the DNA repair protein Chk1. In addition, assessment of a second independent DNA alkylating agent, Carmustine (BCNU), together with DSF-Cu resulted in increased efficacy (Supplementary Fig. S6C) further supporting the idea that DSF-Cu is working at least in part by suppressing DNA repair pathways.

DSF-Cu combined with temozolomide significantly inhibited tumor growth and prolonged survival in patient-derived BTIC intracranial models

As the *in vitro* data indicated that DSF-Cu is cytotoxic in a wide range of patient-derived BTICs and had the ability to enhance the cytotoxic effects of temozolomide *in vitro*, we assessed the clinical applicability of this treatment regime in our well-defined preclinical *in vivo* models (2, 3, 13, 32). For these studies, we chose genetically distinct patient-derived BTICs established from a newly diagnosed (BT134: P53WT, PTENWT, EGFR WT, MGMT

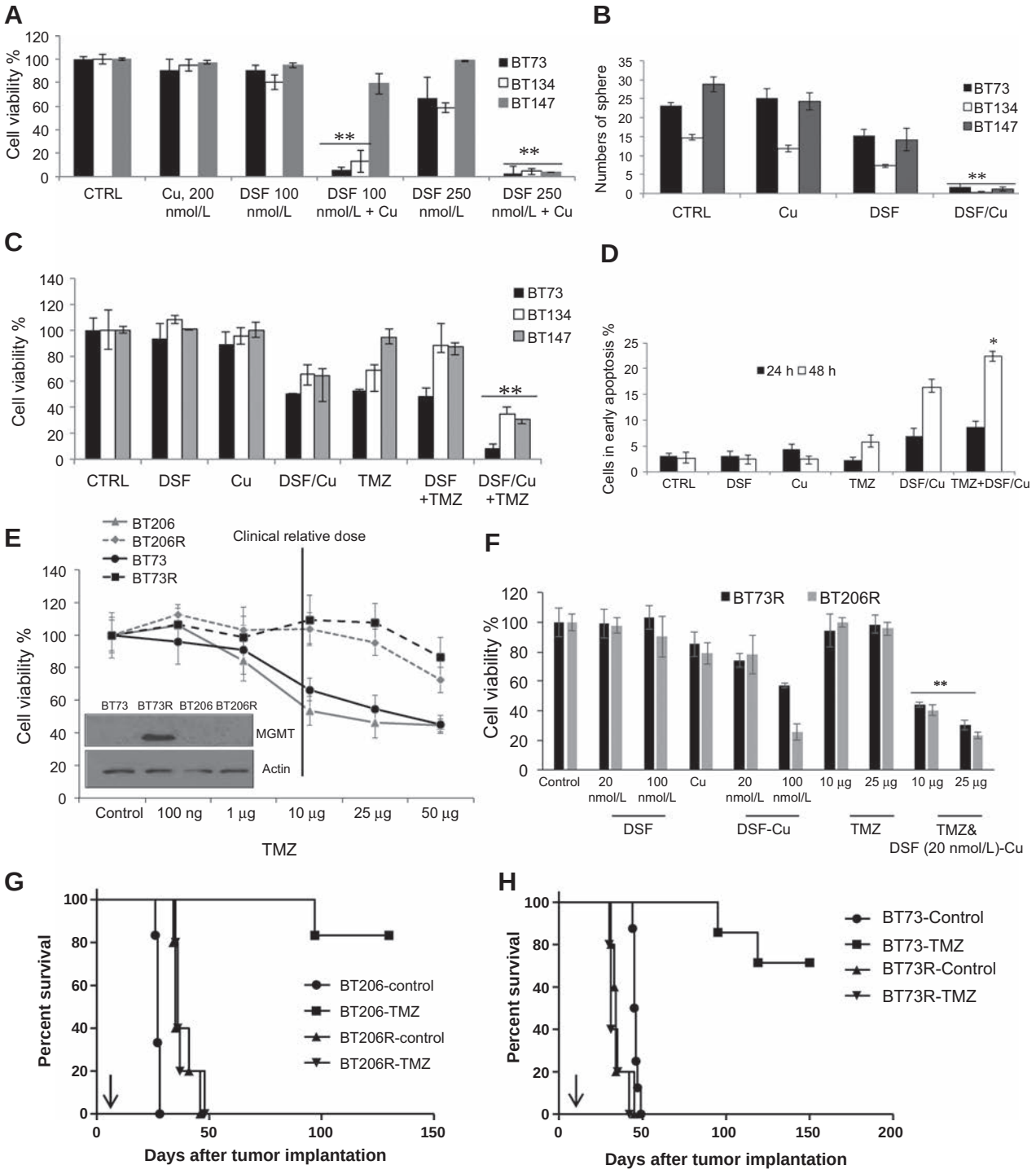

Figure 2.

DSF requires copper for effective killing of genetically distinct patient-derived BTICs, and in combination significantly augments temozolomide (TMZ) cytotoxicity and apoptosis *in vitro.* A, genetically distinct patient-derived BTICs (BT73, BT134, and BT147) were treated with DSF (100 nmol/L or 250 nmol/L) with copper (200 nmol/L) or their combination (DSF-Cu) for 48 hours and assessed for cell viability using AlamarBlue. Graph shows the percentage of viable cells as compared with the untreated control. Double asterisks (**) indicate $P < 0.001$ as compared with the control calculated using Student *t* test. B, self-renewal capacity was examined in the presence of DSF alone (20 nmol/L), Cu alone (200 nmol/L), or DSF-Cu for 7 days. Graph shows the number of secondary spheres formed from 100 viable cells. Double asterisks (**) indicate $P < 0.001$ for DSF-Cu compared with DSF alone calculated using Student *t* test. C, patient-derived BTICs (BT73, BT134, BT147) were treated with DSF alone (20 nmol/L), Cu (200 nmol/L), DSF with Copper (DSF-Cu), temozolomide [10 μg/mL (51.5 μmol/L)], plus DSF alone or DSF-Cu for 7 days and assessed for cell viability using AlamarBlue. Graph shows the percentage of viable cells as compared with the untreated control. Double asterisks (**) indicate $P < 0.001$ as compared with the control calculated using Student *t* test. (*Continued on the following page.*)

unmethylated), recurrent (BT147: P53mut, PTEN$^{-/-}$, EGFRVIII, MGMT unmethylated), and temozolomide-resistant (BT73R) tumors. These BTIC lines exhibited resistance to temozolomide even at high concentrations (10 μg/mL) *in vitro* (Fig. 2E, Supplementary Figs. S4 and S5), thus allowing for the assessment of the DSF-Cu-temozolomide combination therapy *in vivo*. Using intracranial murine xenograft models that had visible tumors by day 7 as assessed by the IVIS-200 Optical *in vivo* imaging system, we randomly assigned animals to the following groups: (i) vehicle control, (ii) temozolomide alone, (iii) DSF-Cu alone; or (iv) temozolomide plus DSF-Cu. Temozolomide and DSF-Cu were given as daily oral administration for 3 cycles (5 days on, 2 days off) at a dose of 30 or 50 mg/kg for temozolomide, 100 mg/kg for DSF, and 2 mg/kg copper (II) gluconate. Animals were monitored every other day and tumor growth was measured at weekly intervals using the IVIS-200 system (total flux emission photons/second). A decrease in tumor burden (signal intensity) was observed in animals treated with the combination therapy (temozolomide plus DSF-Cu). In contrast, no decrease in signal intensity was observed in animals treated with DSF-Cu alone (Fig. 5A and B and Supplementary Fig. S9A and S9B). Quantitative analysis of tumor burden (Fig. 5A and B) demonstrated a consistently smaller tumor burden in the animals treated with DSF-Cu-temozolomide as compared with the continuous increase in tumor burden observed in control animals, DSF-Cu, or temozolomide-treated animals. To confirm the imaging data with respect to an independent measure of tumor burden, 2–3 animals/group were sacrificed 3 weeks following treatment, brains were fixed, paraffin-embedded, and assessed histologically for tumor burden as shown in Supplementary Fig. S10 (top two panels). In addition, whole brain sections were assessed for apoptosis using TUNEL (bottom panel). These data confirmed the *in vitro* results where the combination-based therapy resulted in increased apoptosis as compared with the single agents or control animals (Supplementary Fig. S6D–S6F). Importantly, we demonstrated that while DSF-Cu did not prolong overall survival, and temozolomide had a modest impact in overall survival, the combination of the two drugs had a marked increase in overall survival on newly diagnosed, recurrent, and temozolomide-resistant BTIC intracranial models [Fig. 5A–C; log-rank test, $P < 0.0001$ (Fig. 5A); $P = 0.0006$ (Fig. 5B); $P = 0.0030$ (Fig. 5C)].

To assess the DSF-Cu-temozolomide combination-based therapy in a more clinically relevant formulation, experiments were performed using clinical grade DSF and a copper supplement that can be purchased in many health food stores (copper bisglycinate). Using *in vitro* assays, the combination of copper bisglycinate with DSF was found to be superior to other copper supplements (Centrum Forte; Copper D-gluconate) as assessed by proteasome inhibition (Supplementary Fig. S8C). Most importantly, the clinical grade DSF with copper bisglycinate in combination with temozolomide significantly prolonged survival in animals bearing BT147 intracranial tumors (Supplementary Fig. S9D). Interestingly, using this combination, DSF with copper bisglycinate alone was able to prolong survival, a result that may be consistent with the improved inhibitory activity *in vitro* (Supplementary Fig. S8C). As a surrogate of therapeutic response *in vivo*, we assessed the level of 26S proteasome inhibition in tumor-bearing animals (BT147 and BT73) 5 and 10 days following treatment and found that the ability for DSF to inhibit the 26S activity of the proteasome *in vivo* was enhanced in the presence of the copper supplement, copper bisglycinate, after 10 days of treatment (Fig. 6A).

One hallmark of proteasome inhibition is the induction of an ER stress response; we therefore treated BTICs with DSF-Cu or the clinically approved proteasome inhibitor bortezomib and also assessed for the expression of the ER stress-responsive transcription factor C/EBP homologous protein (CHOP) by Western blot analysis. Treatment with DSF-Cu or bortezomib for 24 hours both resulted in the increased expression of CHOP (Fig. 6B). In addition, and consistent with *in vitro* data, IHC for γ-H2AX in whole brain sections from BT147-bearing animals confirmed *in vivo* the ability of DSF-Cu to enhance the DNA damage induced by temozolomide (Fig. 6C–E). To rule out that the increase in γ-H2AX was not the consequence of an increase in apoptosis, sections were costained for TUNEL and γ-H2AX (Fig. 6E). No significant overlap was observed between nuclear γ-H2AX and TUNEL suggesting that the appearance of γ-H2AX–positive foci is a direct consequence of increased DNA damage and not the result of cells undergoing apoptosis. Collectively, these data show that both γ-H2AX and CHOP increase in response to treatment with DSF-Cu.

Discussion

Despite a deeper molecular understanding of the genetic alterations in human glioma the attempts to translate this information into the clinic through molecularly targeted agents has remained a considerable challenge with very limited success. There are several barriers to effective treatment including tumor heterogeneity, infiltrative nature of the disease, and the lack of many drugs that effectively cross the BBB. We would also argue that many of the cell-based models used for drug screening and assessment may not be predictive and do not account for the complexities of the disease. In recent years, there has been considerable attention to the presence of a stem-like population of glioma cells (4, 5, 46,

(*Continued.*) D, BT147 was treated with DSF (20 nmol/L), Cu (200 nmol/L), DSF-Cu, temozolomide [10 μg/mL, (51.5 μmol/L)] or their combination for 24 or 48 hours, stained with PI and Annexin V, and analyzed using flow cytometry. Graph shows the percentage of cells that were Annexin V–positive indicating cells in early apoptosis. Asterisk (*) indicates $P < 0.05$ for temozolomide/DSF-Cu compared with DSF-Cu or temozolomide alone. E–H, establishment of temozolomide -resistant BTIC variants, BT73R and BT206R. E, graph shows cell viability as assessed by AlamarBlue for BT73, BT206, BT73R, and BT206R after treatment with increasing concentrations of temozolomide [100 ng–50 μg (0.5 μmol/L–257.5 μmol/L)] for 10 days. BT73R and BT206R were established from *in vivo* selection of animals treated with high concentrations of temozolomide (see Materials and Methods). Inset shows Western blot analysis of MGMT expression in BT73 and BT206 parental and resistant (R) variants *in vitro*. F, bar graph shows cell viability as assessed by AlamarBlue for BT73R and BT206R treated with DSF alone (20 nmol/L, 100 nmol/L), Cu (200 nmol/L), DSF with copper (DSF-Cu), temozolomide [10 μg (51.5 μmol/L), 25 μg (128.8 μmol/L)] and temozolomide plus DSF-Cu (20 nmol/L) 7 days after treatment. **, $P < 0.001$ DSF-Cu-temozolomide compared with DSF-Cu or temozolomide alone; Student *t* test. G and H, *in vivo* efficacy of temozolomide on BT73, BT73R, BT206, and BT206R were determined by stereotactically implanting 1×10^5 cells into the right striatum of SCID mice. Tumors were allowed to form for 7 days at which time animals were treated with (i) Oral Plus (control) or (ii) 30 mg/kg temozolomide once per day for 3 cycles (5 days on, 2 days off). Animals were monitored daily. Graphs show Kaplan–Meier survival analysis. $N = 5$–6 animals/group; $P < 0.0001$ for temozolomide as compared with control for BT73 and BT206 while the resistant variants had *P* values equal to 0.09058 (BT73R) and 0.3687 (BT206R) as compared with the control treatment (log-rank test). Arrows indicate the start of temozolomide treatment on day 7.

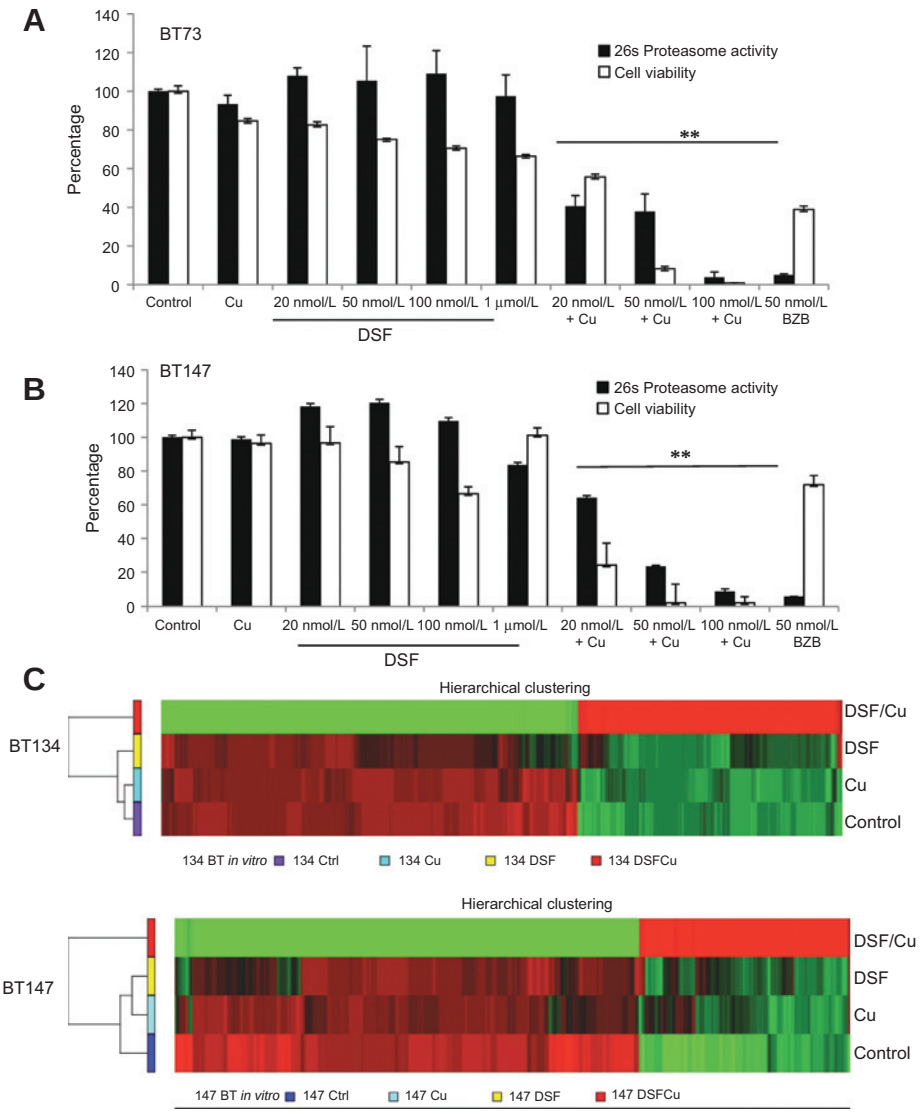

D

Common downregulated DNA repair genes in BT134 and BT147 treated with DSF and copper

DNA damage	Repair mechanisms	Common genes downregulated
Single-strand	Base excision (BER)	BIVM, POLI*, POLH*, POLR2F*, PRMT6, UNG, LIG3*
	Mismatch (MMR)	PMS1*, MSH2,
	Nucleotide excision (NER)	GTF2H4/5*
Double-strand	Non-Homologous end joining (NHEJ)	ATRX*, BRCC3*, DCLRE1A*, ERCC4*, FANCF*, FANCL*, FANCM*,
	Microhomology-mediated end joining (MMEJ)	RAD50, RAD51C*, SMC2, BRCA1*
	Homologous recombination (HR)	ASCC3*, RBM14*, RUVBL1, SHPRH*, USP1, USP10, USP147, NTHL1*

Asterisk indicated (*) genes downregulated *in vivo*

Figure 3.
DSF-Cu inhibits the proteasome and induces global gene expression changes. Patient-derived BTICs (BT73, BT147) were assessed for 26S proteasome chymotrypsin-like activity 24 hours following treatment with DSF (20 nmol/L–100 nmol/L) and DSF with Cu (200 nmol/L). A and B, graphs show the percentage of proteasome activity (black bar) and related cell viability (white bar) as compared with untreated cells (control). Asterisks (**) indicate $P < 0.01$ for proteasome activity of cells treated with DSF-Cu as compared with DSF alone or control (one-way *ANOVA*). The clinically relevant proteasome inhibitor bortezomib (BZB) was used for comparison. C and D, patient-derived BTICs (BT134 and BT147) were treated with 50 nmol/L DSF, 50 nmol/L DSF with 1 μmol/L Cu, Cu alone, or untreated for 12 hours. Cells were lysed and RNA was extracted, purified, labeled using a 3′ IVT Express Kit, and changes in gene expression were assessed using the Affymetrix GeneChip Human PrimeView Array. C, in both BT134 and BT147, DSF with copper treatment resulted in substantial changes in global gene expression as illustrated by the dendrograms showing hierarchical clustering; red indicate upregulated genes and green indicate downregulated genes as compared with controls. D, further data analysis identified a large number of downregulated genes implicated in DNA repair including 29 genes in common between BT134 and BT147. Common downregulated genes are listed in the table along with their associated repair pathway. Asterisks (*) indicated genes downregulated in orthotopic BT147 tumors *in vivo* following DSF-Cu administration. DSF-Cu was given as daily oral administration for 2 cycles (5 days on, 2 days off) at a dose of 100 mg/kg for DSF and 2 mg/kg cooper (II) gluconate.

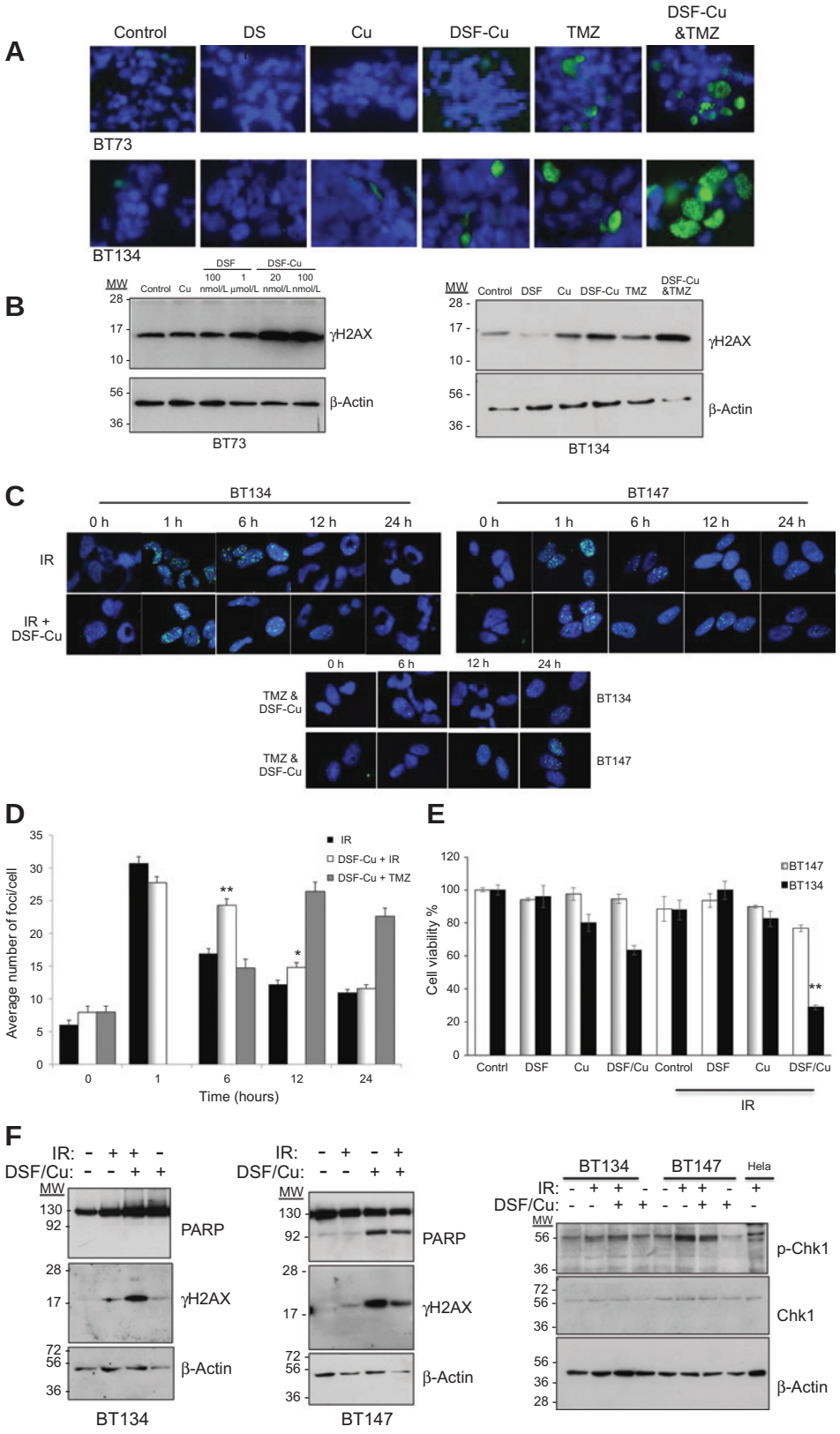

Figure 4.
Temozolomide (TMZ) or IR in combination with DSF-Cu increased/prolonged DNA damage. A and B, patient-derived BT73 and BT134 were treated with saline (control), copper alone (200 nmol/L), DSF (DSF concentrations as indicated), DSF-Cu, temozolomide [10 µg/mL (51.5 µmol/L)], or temozolomide/DSF-Cu for 24 hours. A, shown are representative fluorescent images of BTICs (BT73 and BT134) fixed and stained for γ-H2AX to visualize DNA damage and counterstained with DAPI (blue) to visualize the nuclei. Images were taken at 40× magnification. B, Western blot analysis of γ-H2AX expression confirms the increase in γ-H2AX in BT73 (left) and BT134 (right) in response to DSF-Cu. β-Actin was used as a loading control. C–E, BT134 and BT147 were treated with 2 and 5 Gy IR, or 10 µg/mL (51.5 µmol/L) temozolomide in the absence or presence of DSF-Cu (12-hour pretreatment with 50 nmol/L DSF/200 nmol/L Cu) and assessed for DNA damage at 1, 6, 12, and 24 hours. C, shown are representative images of cells plated on laminin-coated coverslips, treated with 2 Gy IR or temozolomide in the absence or presence of DSF-Cu. Cells were fixed at times indicated and stained for γ-H2AX to visualize DNA damage using fluorescent microscopy. Images were taken at 60× magnification. D, bar graph shows quantitation of the average number of γ-H2AX–positive foci/cell in BT147. Asterisks (**) $P < 0.001$ and $P = 0.01$ for IR plus DSF-Cu compared with IR alone; $P < 0.0001$ for temozolomide compared with control at 6, 12, and 24 hours (Student t test). E, graph shows percentage cell viability of BT134 and BT147 following treatment with saline (control), copper alone (200 nmol/L), DSF (100 nmol/L), or DSF-Cu in the presence or absence of IR (5 Gy). **, $P = 0.0001$ for BT134 IR plus DSF-Cu compared with IR or DSF-Cu alone. F, Western blot analysis using antibodies to phos-Chk1, Chk1, PARP, and γ-H2AX on cell lysates from BT134 and BT147 untreated (control) or treated with 5 Gy IR in the absence or presence of DSF-Cu (12-hour pretreatment with 100 nmol/L DSF/200 nmol/L Cu). Hela cells were used as a positive control for IR and β-Actin was used as a loading control.

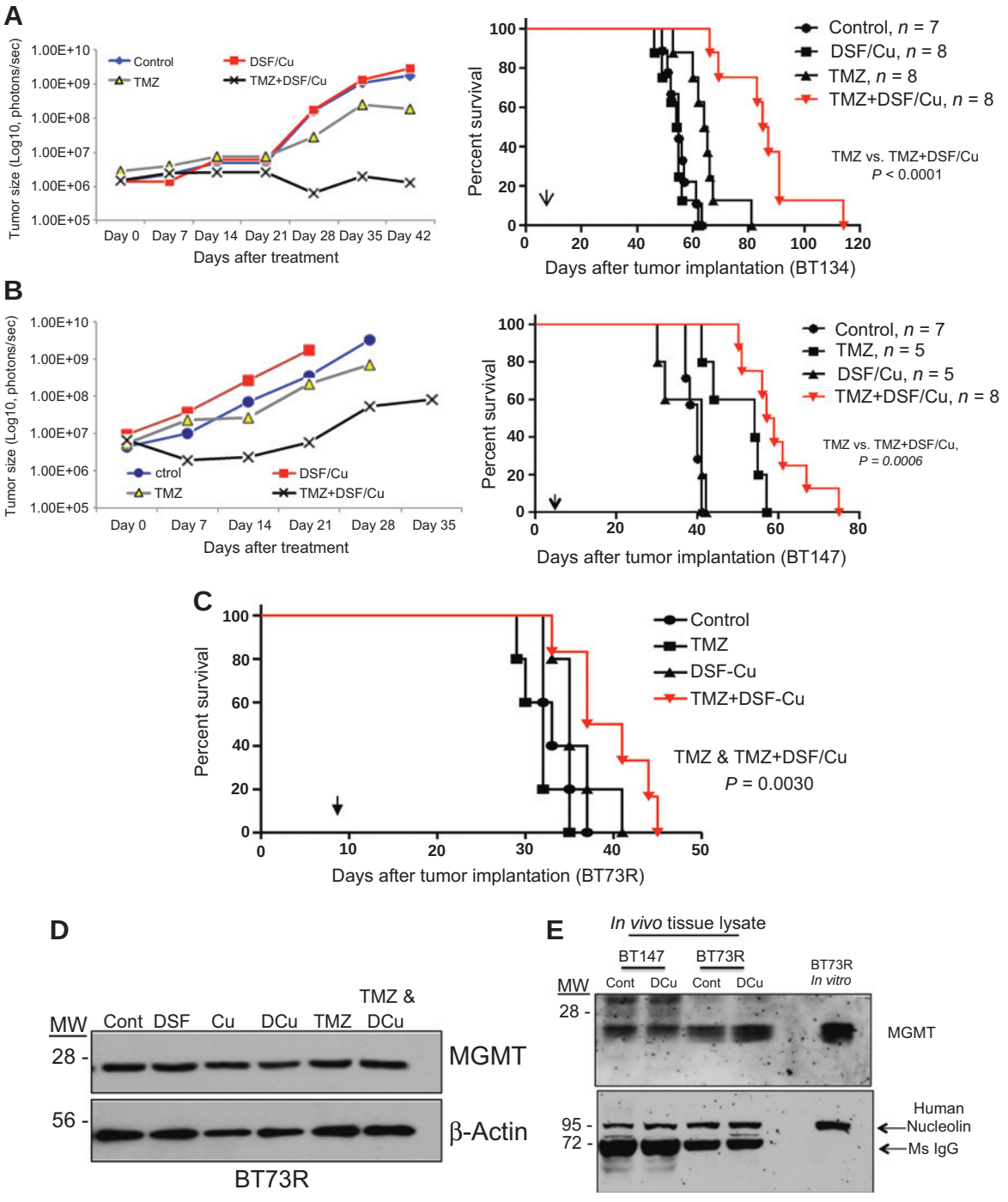

Figure 5.
Temozolomide (TMZ) combined with DSF-Cu inhibits tumor growth and improves survival in patient-derived BTIC intracranial models *in vivo*. Animals bearing intracranial BT134 (A) or BT147 (B) effLuc/eGFP tumors were treated with (i) vehicle control, (ii) temozolomide alone, iii) DSF-Cu alone or iv) temozolomide plus DSF-Cu. Temozolomide and DSF-Cu were given as daily oral administration for 3 cycles (5 days on, 2 days off) at a dose of 50 mg/kg for temozolomide, 100 mg/kg for DSF, and 2 mg/kg cooper (II) gluconate. Animals were monitored every other day and assessed for survival. A and B, tumor growth was measured at weekly intervals using the IVIS-200 Optical *in vivo* imaging system. Graphs (left) show quantitative assessment of tumor burden as analyzed by the IVIS-200 system (Log10, total flux emission photons/second); Animals were monitored for survival (right). Graphs show Kaplan–Meier assessment. $P < 0.0001$ (BT134) and $P = 0.0006$ (BT147) for temozolomide/DSF-Cu as compared with temozolomide alone (log-rank test). N represents the number of animals per group. Arrows indicate the start of treatment. C, *in vivo* efficacy of BT73R following treatment with clinical grade DSF-Cu (100 mg/kg) and copper bisglycinate (2 mg/kg), temozolomide (30 mg/kg) or temozolomide plus DSF-Cu was determined as described above. $N = 5$–7 animals/group; $P = 0.003$ for temozolomide/DSF-Cu as compared with temozolomide alone (log-rank test). Arrow indicates initiation of drug administration. D and E, shown is Western blot analysis of MGMT expression in BT73R following treatment with DSF alone or in combination *in vitro* (D) or *in vivo* (BT73R and BT147; E). β-Actin or human nucleolin (to detect the *in vivo* presence of human tumor cells) were used as loading controls. Binding of the secondary antibody to *in vivo* mouse (Ms) IgG is indicated.

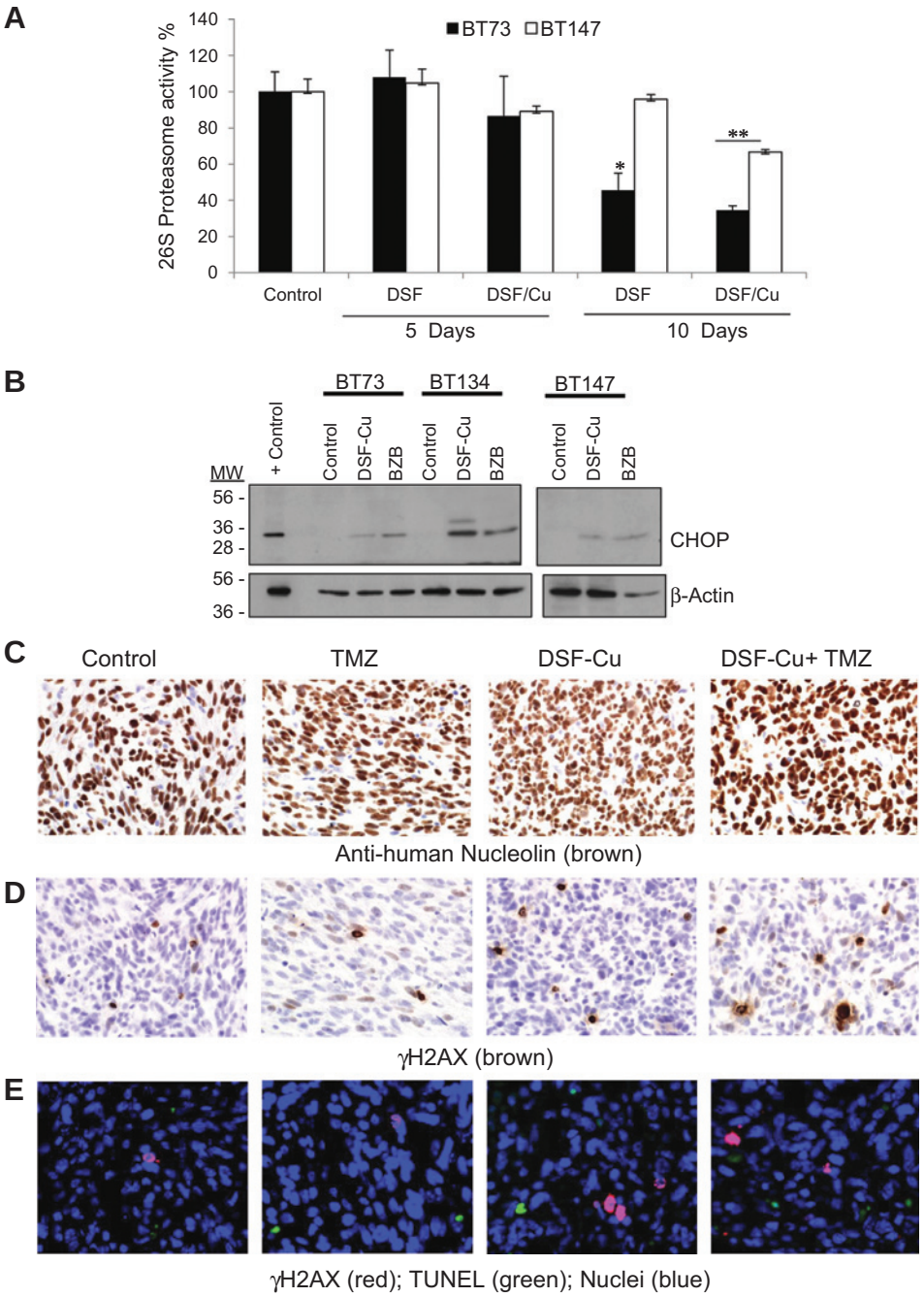

Figure 6.
Assessment of DSF efficacy using clinically relevant markers. A, snap frozen tumor tissue from animals bearing BT73 or BT147 following treatment with DSF (100 mg/kg) or DSF-Cu (100 mg/kg plus 2 mg/kg Cu) for 5 and 10 days were assessed for 26S proteasome chymotrypsin-like activity. Graph shows the percentage of proteasome activity *in vivo* as compared with tumor tissue from control animals treated with Oral Plus. *, $P < 0.05$; **, $P < 0.001$ respectively. B, BT73 and BT147 cells treated with DSF (100 nmol/L) or DSF-Cu (100 nmol/L plus 200 nmol/L Cu) for 24 hours were lysed and proteins were resolved on 12% SDS-PAGE gels. Western blot analysis for the ER stress protein CHOP was performed. The clinically approved proteasome inhibitor bortezomib (BZB; 50 nmol/L) was used for comparison. β-Actin was used as a loading control. C–E, formalin-fixed, paraffin-embedded tissue from animals bearing BT147 following treatment with temozolomide (TMZ; 50 mg/kg), DSF-Cu (100 mg/kg DSF plus 2 mg/kg Cu), or a combination of DSF-Cu/temozolomide for 5 days were stained with anti-human nucleolin (brown; C) to detect the presence of tumor cells; anti-γ-H2AX antibody to detect DNA damage (brown; D), or costained for the presence of apoptosis by TUNEL (green; E), DNA damage by anti-γ-H2AX (red), and DAPI (blue) to visualize the cell nuclei. Sections were counterstained with hematoxylin and images were taken at 60× magnification (C and D) or visualized by fluorescence microscopy (E) at 40× magnification.

47), termed as BTICs, that have been shown to re-populate a tumor (recurrence) and confer resistance to conventional therapies, including temozolomide and radiation (4, 6, 11, 13, 48). In this study, we focused on this population of cells as a model and platform to develop new therapeutic strategies to improve the therapeutic efficacy of standard of care (temozolomide) in the adjuvant setting.

Our focus has been on exploring already marketed (clinically approved) drugs that demonstrate therapeutic potential against the stem-like glioma population. Using a high-throughput *in vitro* drug screen, we found that disulfiram, an off-patent drug previously used to treat alcoholism, in the presence of copper gluconate, or copper bisglycinate, had low nanomolar efficacy against patient-derived BTICs, including the highly infiltrative disease reservoir, *in vitro*. While we found that some glioma lines did not require additional supplemental copper for effective killing, it is clear that in the presence of copper, sensitivity is greatly enhanced, and more importantly, temozolomide resistance can be overcome. In fact, we demonstrate that DSF-Cu can sensitize a completely temozolomide-resistant line to temozolomide. While the exact mechanisms of action for DSF versus DSF-Cu remain unknown we have provided compelling data to suggest that when

combined with copper, DSF is a potent inhibitor of the 26S proteasome as well as an enhancer of DNA-damaging agents due to suppression of DNA repair pathways. Of note, a recent study showed that DSF directly inhibited the expression of MGMT, an enzyme that removes O6 akyl groups from guanine, a repair function in error-free DNA replication (43). However, the reduction of MGMT occurred at concentrations of DSF significantly higher than the IC_{50} of the BTICs. Targeting cancer stem cells (CSC) for better therapeutic outcomes is receiving considerable attention and as ALDH is being used as a biomarker of CSCs, it has been proposed that DSF may be a good therapeutic option (18, 49, 50). However, our data suggest that DSF-Cu is essential for the increased cytotoxicity and ALDH inhibition alone is unlikely to account exclusively for its therapeutic effects *in vitro* and *in vivo*. Our study instead suggests a more global impact for DSF-Cu in affecting proteasome inhibition and DNA repair pathways, and supports the hypothesis that DSF-Cu acts as a multimodality agent in the setting of targeting glioblastoma.

On the basis of a number of features of DSF such as its ability to cross the BBB, low toxicity profile, and its affordability, we believe that DSF-Cu should be tested in glioma patients as an adjunctive treatment to standard of care. MGMT promoter methylation remains the strongest predictive marker for treatment outcome for patients with newly diagnosed glioblastoma (9, 51). It is clear that patients with unmethylated MGMT require better treatment options as their therapeutic benefit to temozolomide is minimal. On the basis of our findings that DSF-Cu is able to enhance the therapeutic effects of temozolomide in both MGMT-positive and MGMT-negative BTICs both *in vitro* and *in vivo* (Figs. 2, 5, and Supplementary Figs. S6 and S7) suggests that unmethylated glioma patients could benefit from the addition of DSF-Cu within their treatment regime. Clearly, the ability to enhance the therapeutic effects of temozolomide and/or BCNU would be advantageous but may come with some added side effects requiring assessment of the toxicity profile of DSF when combined with copper in a phase I study. In addition, we do not know if DSF-Cu targets and/or accumulates preferentially in the glioma cells *in vivo*, and if not, may result in unwanted side-effects in combination with temozolomide, although arguably we have never observed increased toxicity in our preclinical animal models. In addition, based on the results presented here, DSF-Cu may act to enhance the effects of other chemotherapeutic agents used in glioma such as Carmustine and thus warrant assessment of DSF-Cu in combination with other DNA-damaging agents including agents that have shown toxicity in the clinic, as combination with DSF-Cu may allow for a reduction in the dose of the chemotherapy with therapeutic benefit. The notion that DSF-Cu may allow one to lower the amount of temozolomide to gain therapeutic benefit may help reduce both associated toxicities and progression-related mutator phenotypes.

It would certainly be worth considering the use of DSF-Cu in the neoadjuvant and adjuvant setting both in newly diagnosed and recurrent patients as based on the newly described mechanism of action, namely inhibiting DNA repair, DSF-Cu may act as a radiation sensitizer at the time of radiotherapy. Moreover, we believe that our observations are not limited to repurposing DSF solely for glioma but could be used when combined with a copper supplement in a number of cancers for which resistance to DNA-damaging agents is commonly observed and in situations when targeting DNA repair coupled with proteasome inhibition demonstrates therapeutic benefit such as in multiple myeloma (52).

Disclosure of Potential Conflicts of Interest

No potential conflicts of interest were disclosed.

Authors' Contributions

Conception and design: X. Lun, J.C. Wells, J.C. Easaw, J.G. Cairncross, D.R. Kaplan, S.M. Robbins, D.L. Senger

Development of methodology: X. Lun, J.C. Wells, N. Grinshtein, A. Aman, D. Uehling, J.L. Wrana, A. Luchman, D.L. Senger

Acquisition of data (provided animals, acquired and managed patients, provided facilities, etc.): X. Lun, J.C. Wells, N. Grinshtein, J.C. King, X. Hao, N.-H. Dang, X. Wang, A. Aman, D. Uehling, A. Datti, A. Luchman, S. Weiss

Analysis and interpretation of data (e.g., statistical analysis, biostatistics, computational analysis): X. Lun, J.C. Wells, J.C. King, N.-H. Dang, X. Wang, A. Aman, D. Uehling, A. Datti, J.G. Cairncross, S.M. Robbins, D.L. Senger

Writing, review, and/or revision of the manuscript: X. Lun, J.C. Wells, N. Grinshtein, J.C. King, A. Aman, J.C. Easaw, S. Weiss, J.G. Cairncross, D.R. Kaplan, S.M. Robbins, D.L. Senger

Administrative, technical, or material support (i.e., reporting or organizing data, constructing databases): N. Grinshtein, X. Hao, J.L. Wrana, S. Weiss, J.G. Cairncross

Study supervision: D.R. Kaplan, S.M. Robbins, D.L. Senger

Other (PI of program project under which this research was conducted and funded): J.G. Cairncross

Acknowledgments

The authors thank the Brain Tumor Stem Cell Core supported by funds from the Hotchkiss Brain Institute, the Alberta Cancer Foundation, and the Terry Fox Research Institute and the Calgary Brain Tumour and Tissue Bank generously supported by funds from the Clark H. Smith Family. J.C. Wells acknowledges studentship support from the Alberta Cancer Foundation and the University of Calgary. The authors also thank Dr. Aaron Goodarzi and Dr. Anne Vaahtokari from the Arnie Charbonneau Cancer Institute microscopy facility for their assistance and Cortt Piett for his guidance and assistance with the radiation experiments.

Grant Support

This work was supported by the Terry Fox Research Institute Pan-Canadian Translational Research Grant with funds from the Terry Fox Foundation, Alberta Cancer Foundation, Alberta Innovates Health Solutions, and Genome BC (to D.L. Senger, D.R. Kaplan, J.G. Cairncross, S. Weiss, S.M. Robbins) as well as funding from the Canadian Institutes of Health Research (to S.M. Robbins) and the Canadian Stem Cell Network (to D.R. Kaplan and S. Weiss).

The costs of publication of this article were defrayed in part by the payment of page charges. This article must therefore be hereby marked *advertisement* in accordance with 18 U.S.C. Section 1734 solely to indicate this fact.

Received July 27, 2015; revised February 25, 2016; accepted March 11, 2016; published OnlineFirst March 22, 2016.

References

1. Stupp R, Mason WP, van den Bent MJ, Weller M, Fisher B, Taphoorn MJ, et al. Radiotherapy plus concomitant and adjuvant temozolomide for glioblastoma. N Engl J Med 2005;352:987–96.
2. Cusulin C, Chesnelong C, Bose P, Bilenky M, Kopciuk K, Chan JA, et al. Precursor states of brain tumor initiating cell lines are predictive of survival in xenografts and associated with glioblastoma subtypes. Stem Cell Reports 2015;5:1–9.
3. Kelly JJ, Stechishin O, Chojnacki A, Lun X, Sun B, Senger DL, et al. Proliferation of human glioblastoma stem cells occurs independently of exogenous mitogens. Stem Cells 2009;27:1722–33.

4. Bao S, Wu Q, McLendon RE, Hao Y, Shi Q, Hjelmeland AB, et al. Glioma stem cells promote radioresistance by preferential activation of the DNA damage response. Nature 2006;444:756–60.
5. Singh SK, Hawkins C, Clarke ID, Squire JA, Bayani J, Hide T, et al. Identification of human brain tumour initiating cells. Nature 2004; 432:396–401.
6. Beier D, Schulz JB, Beier CP. Chemoresistance of glioblastoma cancer stem cells–much more complex than expected. Mol Cancer 2011;10:128.
7. Galli R, Binda E, Orfanelli U, Cipelletti B, Gritti A, De Vitis S, et al. Isolation and characterization of tumorigenic, stem-like neural precursors from human glioblastoma. Cancer Res 2004;64:7011–21.
8. Salmaggi A, Boiardi A, Gelati M, Russo A, Calatozzolo C, Ciusani E, et al. Glioblastoma-derived tumorospheres identify a population of tumor stem-like cells with angiogenic potential and enhanced multidrug resistance phenotype. Glia 2006;54:850–60.
9. Hegi ME, Diserens AC, Gorlia T, Hamou MF, de Tribolet N, Weller M, et al. MGMT gene silencing and benefit from temozolomide in glioblastoma. N Engl J Med 2005;352:997–1003.
10. Messaoudi K, Clavreul A, Lagarce F. Toward an effective strategy in glioblastoma treatment. Part I: resistance mechanisms and strategies to overcome resistance of glioblastoma to temozolomide. Drug Discov Today 2015;20:899–905.
11. Blough MD, Westgate MR, Beauchamp D, Kelly JJ, Stechishin O, Ramirez AL, et al. Sensitivity to temozolomide in brain tumor initiating cells. Neuro Oncol 2010;12:756–60.
12. Kelly JJ, Blough MD, Stechishin OD, Chan JA, Beauchamp D, Perizzolo M, et al. Oligodendroglioma cell lines containing t(1;19)(q10;p10). Neuro Oncol 2010;12:745–55.
13. Nguyen SA, Stechishin OD, Luchman HA, Lun XQ, Senger DL, Robbins SM, et al. Novel MSH6 mutations in treatment naive glioblastoma and anaplastic oligodendroglioma influence temozolomide resistance independently of MGMT methylation. Clin Cancer Res 2014;20:4894–903.
14. Cen D, Brayton D, Shahandeh B, Meyskens FL Jr, Farmer PJ. Disulfiram facilitates intracellular Cu uptake and induces apoptosis in human melanoma cells. J Med Chem 2004;47:6914–20.
15. Chen D, Cui QC, Yang H, Dou QP. Disulfiram, a clinically used anti-alcoholism drug and copper-binding agent, induces apoptotic cell death in breast cancer cultures and xenografts via inhibition of the proteasome activity. Cancer Res 2006;66:10425–33.
16. Conticello C, Martinetti D, Adamo L, Buccheri S, Giuffrida R, Parrinello N, et al. Disulfiram, an old drug with new potential therapeutic uses for human hematological malignancies. Int J Cancer 2012;131:2197–203.
17. Hothi P, Martins TJ, Chen L, Deleyrolle L, Yoon JG, Reynolds B, et al. High-throughput chemical screens identify disulfiram as an inhibitor of human glioblastoma stem cells. Oncotarget 2012;3:1124–36.
18. Liu P, Brown S, Goktug T, Channathodiyil P, Kannappan V, Hugnot JP, et al. Cytotoxic effect of disulfiram/copper on human glioblastoma cell lines and ALDH-positive cancer-stem-like cells. Br J Cancer 2012; 107:1488–97.
19. Wickstrom M, Danielsson K, Rickardson L, Gullbo J, Nygren P, Isaksson A, et al. Pharmacological profiling of disulfiram using human tumor cell lines and human tumor cells from patients. Biochem Pharmacol 2007;73:25–33.
20. Johansson B. A review of the pharmacokinetics and pharmacodynamics of disulfiram and its metabolites. Acta Psychiatr Scand Suppl 1992;369: 15–26.
21. Borup C, Kaiser A, Jensen E. Long-term Antabuse treatment: tolerance and reasons for withdrawal. Acta Psychiatr Scand Suppl 1992;369:47–9.
22. Cvek B. Targeting malignancies with disulfiram (Antabuse): multidrug resistance, angiogenesis, and proteasome. Curr Cancer Drug Targets 2011;11:332–7.
23. Safi R, Nelson ER, Chitneni SK, Franz KJ, George DJ, Zalutsky MR, et al. Copper signaling axis as a target for prostate cancer therapeutics. Cancer Res 2014;74:5819–31.
24. Westhoff MA, Zhou S, Nonnenmacher L, Karpel-Massler G, Jennewein C, Schneider M, et al. Inhibition of NF-kappaB signaling ablates the invasive phenotype of glioblastoma. Mol Cancer Res 2013;11:1611–23.
25. Yip NC, Fombon IS, Liu P, Brown S, Kannappan V, Armesilla AL, et al. Disulfiram modulated ROS-MAPK and NFkappaB pathways and targeted breast cancer cells with cancer stem cell-like properties. Br J Cancer 2011;104:1564–74.
26. Kona FR, Buac D, A MB. Disulfiram, and disulfiram derivatives as novel potential anticancer drugs targeting the ubiquitin-proteasome system in both preclinical and clinical studies. Curr Cancer Drug Targets 2011; 11:338–46.
27. Brar SS, Grigg C, Wilson KS, Holder WD Jr, Dreau D, Austin C, et al. Disulfiram inhibits activating transcription factor/cyclic AMP-responsive element binding protein and human melanoma growth in a metal-dependent manner in vitro, in mice and in a patient with metastatic disease. Mol Cancer Ther 2004;3:1049–60.
28. Zemp FJ, Lun X, McKenzie BA, Zhou H, Maxwell L, Sun B, et al. Treating brain tumor-initiating cells using a combination of myxoma virus and rapamycin. Neuro Oncol 2013;15:904–20.
29. Rabinovich BA, Ye Y, Etto T, Chen JQ, Levitsky HI, Overwijk WW, et al. Visualizing fewer than 10 mouse T cells with an enhanced firefly luciferase in immunocompetent mouse models of cancer. Proc Natl Acad Sci U S A 2008;105:14342–6.
30. Grinshtein N, Datti A, Fujitani M, Uehling D, Prakesch M, Isaac M, et al. Small molecule kinase inhibitor screen identifies polo-like kinase 1 as a target for neuroblastoma tumor-initiating cells. Cancer Res 2011;71: 1385–95.
31. Smith KM, Datti A, Fujitani M, Grinshtein N, Zhang L, Morozova O, et al. Selective targeting of neuroblastoma tumour-initiating cells by compounds identified in stem cell-based small molecule screens. EMBO Mol Med 2010;2:371–84.
32. Wang L, Rahn JJ, Lun X, Sun B, Kelly JJ, Weiss S, et al. Gamma-secretase represents a therapeutic target for the treatment of invasive glioma mediated by the p75 neurotrophin receptor. PLoS Biol 2008;6:e289.
33. Ahn BY, Saldanha-Gama RF, Rahn JJ, Hao X, Zhang J, Dang NH, et al. Glioma invasion mediated by the p75 neurotrophin receptor (p75/CD271) requires regulated interaction with PDLIM1. Oncogene 2016;35:1411–22.
34. Johnston AL, Lun X, Rahn JJ, Liacini A, Wang L, Hamilton MG, et al. The p75 neurotrophin receptor is a central regulator of glioma invasion. PLoS Biol 2007;5:e212.
35. Reynolds BA, Tetzlaff W, Weiss S. A multipotent EGF-responsive striatal embryonic progenitor cell produces neurons and astrocytes. J Neurosci 1992;12:4565–74.
36. De Lepeleire I, Reiss TF, Rochette F, Botto A, Zhang J, Kundu S, et al. Montelukast causes prolonged, potent leukotriene D4-receptor antagonism in the airways of patients with asthma. Clin Pharmacol Ther 1997;61:83–92.
37. Reiss TF, Sorkness CA, Stricker W, Botto A, Busse WW, Kundu S, et al. Effects of montelukast (MK-0476); a potent cysteinyl leukotriene receptor antagonist, on bronchodilation in asthmatic subjects treated with and without inhaled corticosteroids. Thorax 1997;52:45–8.
38. Richards DA. Prophylactic value of clioquinol against travellers' diarrhoea. Lancet 1971;1:44–5.
39. Cvek B. Nonprofit drugs as the salvation of the world's healthcare systems: the case of Antabuse (disulfiram). Drug Discov Today 2012;17:409–12.
40. Choi SA, Choi JW, Wang KC, Phi JH, Lee JY, Park KD, et al. Disulfiram modulates stemness and metabolism of brain tumor initiating cells in atypical teratoid/rhabdoid tumors. Neuro Oncol 2015;17:810–21.
41. Kast RE, Halatsch ME. Matrix metalloproteinase-2 and -9 in glioblastoma: a trio of old drugs-captopril, disulfiram and nelfinavir-are inhibitors with potential as adjunctive treatments in glioblastoma. Arch Med Res 2012;43:243–7.
42. Triscott J, Lee C, Hu K, Fotovati A, Berns R, Pambid M, et al. Disulfiram, a drug widely used to control alcoholism, suppresses the self-renewal of glioblastoma and over-rides resistance to temozolomide. Oncotarget 2012;3:1112–23.
43. Paranjpe A, Zhang R, Ali-Osman F, Bobustuc GC, Srivenugopal KS. Disulfiram is a direct and potent inhibitor of human O6-methylguanine-DNA methyltransferase (MGMT) in brain tumor cells and mouse brain and markedly increases the alkylating DNA damage. Carcinogenesis 2014; 35:692–702.
44. Kreklau EL, Kurpad C, Williams DA, Erickson LC. Prolonged inhibition of O(6)-methylguanine DNA methyltransferase in human tumor cells by O (6)-benzylguanine in vitro and in vivo. J Pharmacol Exp Ther 1999;291: 1269–75.

45. Veverka KA, Johnson KL, Mays DC, Lipsky JJ, Naylor S. Inhibition of aldehyde dehydrogenase by disulfiram and its metabolite methyl diethylthiocarbamoyl-sulfoxide. Biochem Pharmacol 1997;53:511–8.
46. Hemmati HD, Nakano I, Lazareff JA, Masterman-Smith M, Geschwind DH, Bronner-Fraser M, et al. Cancerous stem cells can arise from pediatric brain tumors. Proc Natl Acad Sci U S A 2003;100:15178–83.
47. Vescovi AL, Galli R, Reynolds BA. Brain tumour stem cells. Nat Rev Cancer 2006;6:425–36.
48. Chen J, Li Y, Yu TS, McKay RM, Burns DK, Kernie SG, et al. A restricted cell population propagates glioblastoma growth after chemotherapy. Nature 2012;488:522–6.
49. Moreb JS, Ucar D, Han S, Amory JK, Goldstein AS, Ostmark B, et al. The enzymatic activity of human aldehyde dehydrogenases 1A2 and 2 (ALDH1A2 and ALDH2) is detected by Aldefluor, inhibited by diethylaminobenzaldehyde and has significant effects on cell proliferation and drug resistance. Chem Biol Interact 2012;195:52–60.
50. Landen CN Jr, Goodman B, Katre AA, Steg AD, Nick AM, Stone RL, et al. Targeting aldehyde dehydrogenase cancer stem cells in ovarian cancer. Mol Cancer Ther 2010;9:3186–99.
51. Hegi ME, Stupp R. Withholding temozolomide in glioblastoma patients with unmethylated MGMT promoter–still a dilemma? Neuro Oncol 2015;17:1425–7.
52. Gourzones-Dmitriev C, Kassambara A, Sahota S, Reme T, Moreaux J, Bourquard P, et al. DNA repair pathways in human multiple myeloma: role in oncogenesis and potential targets for treatment. Cell Cycle 2013;12:2760–73.